АГРОХИМИЯ И АГРОПОЧВОВЕДЕНИЕ

AGROCHEMISTRY AND AGRICULTURAL SOIL SCIENCE

DOI: 10.12731/2658-6649-2025-17-3-1035 **EDN: KTSAMQ**
UDC 631.4:004.94

Original article

USING HYDRUS-1D SOFTWARE TO PREDICT CUMULATIVE INFILTRATION VALUES FOR DIFFERENT SOIL TEXTURES

F.A. Al-Wazzan

Abstract

Four soil samples with varying textures (clay loam, clay, sandy clay loam, and silty loam) were collected from different locations in Nineveh Governorate, northern Iraq. Four different models were used to calculate air-entry values, including Lenhard (Ψ_e), Cornelis (Ψ_{e1}), Van Genuchten (Ψ_{e2}), and a modified model proposed in this study ($\Psi_{e.m}$) and a modified model proposed in this study (α). These values, which represent the inverse of the air-entry value (α), serve as inputs for the Hydrus-1D program. It is a difficult standard to measure and requires time and work to estimate. These models were used in the Brooks and Corey model (1964) to predict accumulated infiltration. It is expressed in the following formulas ($I_{\Psi e}$, $I_{\Psi e1}$, $I_{\Psi e2}$, $I_{\Psi em}$). As a new method in predicting accumulated infiltration values by using the Hydrus-1D program and comparing it with infiltration values measured in the laboratory and field. This a novel scientific enhances the program's functionality and updates input data to minimize errors.

The results demonstrated that cumulative infiltration predicted by Hydrus-1D using hydraulic functions (θ_s, θ_r, K_s) and the two constants in V.G model (*α, n,*) gave close values to the measured values. A high level of agreement was also observed between the predicted accumulated infiltration values ($I_{\Psi e}$, $I_{\Psi e1}$, $I_{\Psi e2}$, $I_{\Psi em}$) and the measured values when the same program was used, relying on the air-entry values of (Ψ_e, Ψ_{e1}, Ψ_{e2}, $\Psi_{e.m}$) as an alternative to the (α) value. The modified value in this study

($\Psi_{e.m}$) gave the best results to predict accumulated infiltration values when used in the Hydrus-1D program. We recommend adopting this modified value (Ψe.m) in Hydrus-1D to predict soil hydraulic properties.

Keywords: accumulative infiltration; accumulated infiltration prediction; soil hydraulic parameters; Hydrus-1D program

For citation. Al-Wazzan, F. A. (2025). Using Hydrus-1D software to predict cumulative infiltration values for different soil textures. *Siberian Journal of Life Sciences and Agriculture*, *17*(3), 283-299. https://doi.org/10.12731/2658-6649-2025-17-3-1035

Introduction

Understanding water and solute transport in unsaturated soil is a complex yet critical topic. It poses significant challenges for researchers in soil and irrigation sciences, requiring considerable time and effort and being influenced by environmental conditions. Mathematical models describing water movement through porous soil media are essential for quantifying hydraulic properties that provide a quantitative description and accurate explanations of the water functions and the detailed knowledge about the constants of these functions in order to take action against the lack of soil moisture and to reach better methods for irrigation water scheduling and management [1].

Modern approaches employ mathematical models to predict soil water characteristics, including infiltration and unsaturated hydraulic conductivity, and the accuracy of these equations depends largely on the water functions, such as the saturation moisture content (θ_s) the residual moisture content (θ_r) and the water function constants represented by the Van Genuchten constants (α, *n* and *m*).

Many attempts have been made to estimate these functions and their constants to simulate the movement of the water within the porous medium of soil, as researchers have used various methods based on the numerical solutions of Richards equation of unsaturated flow to develop mathematical models to predict some water functions of the soil that presented a Clear perception that describes the unsaturated flow under the lab conditions and developing them led to the natural use in the field conditions. The huge development on programming abilities resulted in using multiple programs to predict different characteristics. The Hydrus-1D software is considered one of the most important software for simulating the movement and transfer of water, salts and heat in one dimension in saturated and unsaturated porous media. The numerical solution of Richard's equation and the mathematical models, that predict some water soil properties like the moisture description curve; in order to fit the measurement in the software and they simulate the basic soil properties and represent the best natural prediction method [2]. Also, the Hydrus-1D software is related to Marquardt-Levenberg algorithm to find the inverse solutions to predict the hydraulic constants depending on other characteristics like evaporation [3; 4; 5] indicating that when using Hydrus-1D software in their study to the changing conditions of the moisture content during the flow process of two soils; one of them is sandy loam and the other is loam sand to a high degree of compatibility between the values measured and the values predicted by the software in addition to the possibility of detecting the water movement within the porous medium.

Infiltration is very important in designing the irrigation systems, managing its operations and evaluating its efficiency as it expresses the access of water to the soil through the surface due to adding water by irrigation or the rain and it takes place due to the integration of the water conductivity and the decline of the water potential at the surface of the soil [6]. There are many factors that affect infiltration to the soil, the most important is the initial moisture content ($\theta_0 \theta_0$) and influence appears within the first (20) minutes of infiltration in addition to the soil texture, its porosity and the extent to which the air is detained inside the pores and the type of soil structure. Also, the physical properties of the soil play an important role in the process of infiltration [7].

The Philip equation [8] is regarded as the most important equation that describes the accumulative infiltration:

$$D = St^{0.5} + At \quad (1)$$

Where D = The accumulative infiltration, cm, S = sorptivity, t: time, min, A = constant

The factor (A) is connected to the water soil properties, the earth gravity and the time which is considered the influential factor in water infiltration. It is observed that absorptivity has an effect on water infiltration in the soil in short time and responsible for moving the water in the early stages of the infiltration and after that the absorptivity role becomes less influential and role of the factor (A) becomes more obvious with longer periods of time until reaching the balance of the water quantity that enters the soil in the time unit.

The equation of Kostiyakov that describes the infiltration in the soil is regarded as an experimental equation and one of the simple models that is easily applied therefore it has been used in the study and evaluation of the various irrigation systems.

$$D = at^{b} \quad (2)$$

Where D = accumulative infiltration (cm), t = time (min), a and b = constants of Kostiyakov equation that is estimated from the infiltration data.

The previous equation used for estimating the infiltration involves many weaknesses that are represented by incapability of calibrating or modifying them to suit the condition other than the ones it measured the infiltration within them, and this entails conducting the field tests again to collect the infiltration data and this requires tremendous amount of time consumed and efforts to be made.

Materials and methods

Disturbed and undisturbed soil samples were collected from the surface layer (0–30 cm depth) at four sites in Nineveh Governorate, northern Iraq. The soils are various textures in areas of Nineveh governorate which are considered with the arid and semi-arid areas in the north of Iraq. The soils are calcareous, with the majority classified as Calciorthids according to the American Soil Classification System. The samples were taken to the lab after they were dried, ground, and sieved with a 2-mm sieve to be ready for the physical and chemical analytics [9].

Table 1.

Some physical properties of the soil

Soil type	Order	Soil particle fractions gm. Kg^{-1}			Soil Organic Matter	Total porosity	Bulk density	Hydraulic conductivity	Initial Volumetric water content
		Clay	silt	sand	gm. kg-1	cm.cm^{-1}	Mg. m^{-3}	cm. hr^{-1}	cm.cm^{-3}
Clay loam	**ENTISOLS**	**300**	**461**	**239**	**11.33**	**0.48**	**1.36**	**0.158**	**0.182**
Clay	**ARIDISOLS**	**570**	**315**	**115**	**22.65**	**0.528**	**1.25**	**0.069**	**0.20**
Sandy clay loam	**ENTISOLS**	**225**	**240**	**535**	**5.18**	**0.486**	**1.36**	**0.360**	**0.130**
Silty loam	**ARIDISOLS**	**240**	**560**	**200**	**9.92**	**0.505**	**1.31**	**0.222**	**0.177**

Table 2.

Some chemical properties of the soil

Property	Texture				Unit
	Clay loam	Clay	Sandy clay loam	Silty loam	
pH	**8.23**	**8.39**	**7.95**	**7.84**	
EC	**0.63**	**1.72**	**0.75**	**3.42**	**dSm^{-1}**
Na exchanged	**0.88**	**2.55**	**1.00**	**3.77**	**Cmolc kg^{-1}**
CEC	**24**	**30**	**18**	**26**	
Total carbonate	**316**	**405**	**289**	**290**	**g kg^{-1}**

Water infiltration

Field measurements

Measurements of water infiltration in the soils of the study area were conducted in four sites using the double-ring infiltrometer according to the method described by [10]. The inner ring had a diameter of 30 cm, while the outer ring measured 60 cm in diameter, and both have a height of 60 cm.

The small ring was fixed inside the bigger one in a depth of 10 cm from the soil surface and the float was connected inside the small ring and connected with a plastic tube that is connected to a 80-cm-height rectangular metal tank with a diameter that equals the diameter of the small ring to supply water and on the rings side a graded glass tube is fixed vertically to measure the infiltrated water with the time for the soils of the four sites.

Laboratory measurements

The vertical infiltration was measured in the laboratory in the columns of the soils with various textures for all the sites studies by means of using a plastic column with a diameter of 6 cm and a height of 14 cm. These were filled with soil at an apparent density that is similar to the field soil and the infiltrated water was measured with time.

Use of Hydrus-1D software

The principle of the software is summarized with a numerical solution of a differential equation with physical bases. The data is entered in a group of lists that are fed depending on the property studied.

Theoretical basis

The theoretical basis of Hydrus-1D software relies on the numerical solution of the water flow equation, assuming an incompressible medium. It is based on Darcy's law equation, represented by Richards equation, which describes one-dimensional water flow:

$$\frac{\partial \theta}{\partial t} = \frac{\partial}{\partial x}\left[K\left(\frac{\partial h}{\partial x} + \cos\alpha\right)\right] - S \qquad (3)$$

Where θ = the moisture content (cm^3), h = moisture stress (cm water), t = time, S = term that represents the collection and supply of water in the flow equation ($cm^3.cm^3.min^{-1}$).

Modifying the air-entry value parameter (α) in Hydrus-1D:

The value of the constant (α) was modified, which stands for the inverse of the value of air entry using four different models to show its effect on the software outputs and a new style to manifest the effect of this constant modifying according to the outputs of the software and then comparing the predicted values with the measured ones for a varying domain of soil textures.

The air-entry pressure was found in four formulas as follows:

A - Lenhard formula (ψ_e), and mentioned in [11]:

$$\psi_e = 0.5^{\frac{1}{\lambda}}(2^{\frac{1}{m}} - 1)^{\frac{1}{n}} \quad (4)$$

B - In this study the Lenhard formula (ψ_e) was modified by changing the constant from (0.5) to (1.2) and the symbol was given to it (ψ_{em})

$$\psi_{e_m} = 1.20^{\frac{1}{\lambda}}(2^{\frac{1}{m}} - 1)^{\frac{1}{n}} \quad (5)$$

C - The formula of Cornelis (ψ_{e1}) and mentioned in [12]:

$$\psi_{e1} = \frac{1}{0.5\alpha} \quad (6)$$

D - The formula of van Genuchten (ψ_{e2}) It was mentioned in13]].

$$\psi_{e2} = \frac{1}{\alpha} \quad (7)$$

Results and discussion

Accumulative water infiltration measured in the field

The values of the accumulative water infiltration measured in the field were 1.11, 0.940, 3.087 and 1.7 cm compared to the values measured in the laboratory, which were 1.072, 0.912, 2.945 and 1.66 cm respectively after 200 min from the measurement, Tables 3 and 4. This is attributed to the soil, which preserves its structure and its aggregations stability in the field sites and because there were cracks and remains of roots that helped increase the depth of the infiltrated water. On the other hand, the laboratory soil was disturbed, leading to structural breakdown. This is in conformity with the results of the [14; 15; 16] confirming that the accumulative infiltration values measured in the field are higher than the ones measured in the laboratory. The lowest cumulative infiltration value measured in clay-textured soil was 0.940 cm. since these soils have small pores and have the ability to preserve moisture and thus the ability of water conductivity and the movement of water in both vertically and horizontally slow. The highest value of field accumulative infiltration was at the site with sandy clay loam texture, i.e., 3.087 cm. This can be attributed to the lower clay content and higher sand content, which increases the cross-sectional area for water flow through the porous medium, thereby enhancing infiltration. This is conformity with the results of [17] that indicated that the soils with light texture have high infiltration values.

Values of the accumulative infiltration measured in the laboratory

It was shown that the lowest values of the accumulative infiltration measured in the laboratory were in clay-textured soils as he reached0.911 cm at 200 min later. The reason for this is the decrease in the cumulative infiltration values in the fine textured soils. It is due to the compaction of the soil and the confinement of the air, causing the opposite pressure and swelling of the clay particles, which leads to a small size of the interstitial pores as well as the movement and transmission of fine particles and their deposition within the interfacial pores, reducing the movement of water to the bottom.

Values of the accumulative infiltration predicted by HYDRUS-1D

Richards equation was solved by means of the numerical method using the ended elements by applying Hydrus and the water functions (θ_s, θ_r, K_S) and the two constants (α and *n*) in [13].

The solution process to obtain the predicted accumulative infiltration values is represented by b (I_v). Also, the same water functions were used with the calculated of air entry values from the equations (4, 5, 6, 7), as a tool for improving the method of predicting the accumulative infiltration values represented by ($I\psi_e$, $I\psi_{e_m}$, $I\psi_{e_1}$, $I\psi_{e_2}$), respectively. Predicted cumulative infiltration values closely matched field-measured values, with a Nash-Sutcliffe efficiency (NSE) ranging from 0.939 to 0.999 for all the sites (Table 3). The limiting values ranged from 0.939 to 0.999 and the lowest value was in the sandy clay loam and the highest was in the silty loam soil, while the value of RMSE was 0.0553 in the silty loam to 3.9375 in the sandy clay loam. Table 3 and Fig. 1 show the relationship between these values. The predicted values of accumulative infiltration (I_v) were closer with the measured values. The values of the statistical significance that the highest value was 0.999 and the lowest value for the RMSE. From the other hand $I\psi_{e_m}$) of the accumulative infiltration showed closer values compared to the other equation, depending of air entry value. Results in Table 4 showed that the predicted values of accumulative infiltration were close to the values measured at the laboratory in all the soils of the study. The value of limitation coefficient ranged from 0.025 to 0.999 and the lowest value was in the clay soil and the value of RMSE was 0.0035 in the clay soil. The accumulation infiltration predicted values (I_v) were closer to the measured values and this might be due to that some predicted values (I_v) depended on the measurement and the accurate estimation of the water functions and the constants (α and *n*), whereas the values of the accumulated infiltration predicted by $I\psi_e$, $I\psi_{e_m}$, $I\psi_{e_1}$, $I\psi_{e_2}$) were less convergent to the measured values and this might be because the values predicted depended on air entry values calculated from predictive equation and this yielded more accuracy in the direct measurements. The lowest predicted values of the accumulative infiltration were ($I\psi_e$) compared to the values measured and the values of the other predicted accumulative infiltration, Fig. 2 due to the decrease of the value of air entry (ψ_e) were calculated in the Equation 4, which led to the rise in the constant values (α). The ($I\psi_{e_m}$) of predicting the accumulative infiltration showed values that are more compatible with the values measured compared to ($I\psi_e$) for all the soil in question and the reason behind that is the modification of equation (4) in this study by changing the constant of the equation from 0.5 to 1.2 (Equation 5) and this in turn resulted in an increase in the values of air entry, which decreased the value of the constant (α) and so better results were provided by Hydrus-1D. This way the sensitivity of ($I\psi_e$) was treated at or close to the saturation of the clay soils as the identification coefficient of the site with clay texture was 0.997 as noted in Table 4 and Fig. 3. The air entry value in ($I\psi_{e_1}$) and ($I\psi_{e_2}$) was calculated depending on the measured value of (α). The model ($I\psi_{e_1}$) showed the highest predicted values of accumulative infiltration for all the soils of the sites in question (Table 4). That was because the air entry value reached the maximum when calculated from the relation ($\frac{1}{0.5\alpha}$) as well as the decrease in the value of (α). That reached the maximum, which is in agreement with the results [18].

The predicted values of the accumulative infiltration in ($I\psi_{e_2}$) showed more compatibility with the values measured and they were close to the predicted values of the mode ($I\psi_{e_m}$) (Fig. 3) as it was the lowest value for the identification coefficient of the clay texture and the reason behind that is due to the rise in the value of air entry (ψ_e), which was calculated from the relation ($\frac{1}{\alpha}$) and this led to a decrease in (α) value and this was indicated by [4; 11; 19], which demonstrated the inverse relation between the air entry value and the factor (α). It was noticed that the predicted values of the accumulated infiltration increased when using the two models ($I\psi_{e_1}$) and ($I\psi_{e_2}$) using the Hydrus-1D software at the long periods of time (i.e., 160 and 200 min) and the occurrence of a slight change to the values when compared with the measured values. This is in agreement with what was indicated by [20; 21; 22; 23], which indicated that there is a possibility for the occurrence of a slight deviation in the predicted values when using the prediction equations for the accumulative infiltration at the end of the measurement periods due to the factor of time and these deviations will be according to the model used.

Table 3.

Accumulated infiltration values field-measured and predicted by the Hydrus-1D

			accu-mulated	**infiltra-tion**	**predic-tion**	**By Hy-drus**	**Cm**
	Time, min	**Accumulated infil-tration field-mea-sured, cm**	I_V	$I\psi_e$	$I\psi_{em}$	$I\psi_{e1}$	$I\psi_{e2}$
Clay loam	1	0.181	0.153	0.022	0.086	0.098	0.077

Clay	1	0.166	0.152	0.017	0.076	0.105	0.068
Sandy clay loam	1	0.293	0.287	0.024	0.201	0.247	0.111
Silty loam	1	0.193	0.180	0.022	0.126	0.157	0.078
Clay loam	3	0.246	0.217	0.030	0.151	0.166	0.144
Clay	3	0.227	0.208	0.025	0.124	0.166	0.118
Sandy clay loam	3	0.437	0.433	0.043	0.375	0.452	0.367
Silty loam	3	0.285	0.269	0.041	0.209	0.285	0.136
Clay loam	7	0.311	0.281	0.055	0.233	0.258	0.207
Clay	7	0.284	0.269	0.041	0.198	0.276	0.182
Sandy clay loam	7	0.635	0.616	0.077	0.586	0.705	0.542
Silty loam	7	0.387	0.370	0.056	0.317	0.442	0.206
Clay loam	10	0.352	0.317	0.066	0.278	0.310	0.245
Clay	10	0.321	0.296	0.053	0.233	0.317	0.212
Sandy clay loam	10	0.743	0.721	0.091	0.703	0.856	0.692
Silty loam	10	0.443	0.427	0.073	0.374	0.524	0.245
Clay loam	20	0.435	0.413	0.095	0.382	0.434	0.344
Clay	20	0.401	0.374	0.075	0.317	0.448	0.295
Sandy clay loam	20	1.023	0.994	0.144	1.012	1.208	1.006
Silty loam	20	0.578	0.565	0.111	0.522	0.741	0.353
Clay loam	30	0.496	0.477	0.122	0.466	0.536	0.423
Clay	30	0.452	0.428	0.092	0.392	0.552	0.356
Sandy clay loam	30	1.356	1.204	0.198	1.258	1.503	1.248
Silty loam	30	0.687	0.685	0.147	0.652	0.915	0.446
Clay loam	90	0.772	0.743	0.277	0.820	0.977	0.752
Clay	90	0.683	0.653	0.185	0.703	0.975	0.626
Sandy clay loam	90	2.121	2.066	0.494	2.285	2.671	2.274
Silty loam	90	1.136	1.126	0.364	1.147	1.615	0.833
Clay loam	160	1.012	0.970	0.446	1.113	1.356	1.031
Clay	160	0.857	0.835	0.279	0.960	1.328	0.849
Sandy clay loam	160	2.892	2.776	0.844	3.145	3.623	3.132
Silty loam	160	1.520	1.503	0.606	1.573	2.196	1.186
Clay loam	200	1.11	1.080	0.542	1.254	1.547	1.170
Clay	200	0.940	0.922	0.331	1.087	1.498	0.957
Sandy clay loam	200	3.087	3.1226	1.043	3.578	4.092	3.556

Silty loam	200	1.7	1.686	0.744	1.784	2.481	1.367
Clay loam		R^2 **RMSE**	0.999 0.107	0.950 1.329	0.990 0.057	0.986 0.296	0.989 0.216
Clay		R^2 **RMSE**	0.999 0.0773	0.952 1.312	0.980 0.107	0.981 0.531	0.983 0.270
Sandy clay loam		R^2 **RMSE**	0.996 0.171	0.939 3.937	0.994 0.187	0.996 1.087	0.994 0.101
Silty loam		R^2 **RMSE**	0.999 0.055	0.952 1.955	0.997 0.112	0.997 0.966	0.991 0.869

Table 4.

Accumulated infiltration values laboratory-measured and predicted by the Hydrus-1D

			accu-mulated	**infiltra-tion**	**predic-tion**	**By Hy-drus**	**Cm**
	Time, min	**Lab-measured accumulated infil-tration, cm**	I_V	$I\psi_e$	$I\psi_{em}$	$I\psi_{e1}$	$I\psi_{e2}$
Clay loam	1	0.135	0.151	0.026	0.078	0.105	0.077
Clay	1	0.133	0.145	0.012	0.067	0.096	0.071
Sandy clay loam	1	0.220	0.274	0.024	0.102	0.307	0.215
Silty loam	1	0.152	0.178	0.017	0.076	0.158	0.117
Clay loam	3	0.202	0.218	0.044	0.137	0.190	0.136
Clay	3	0.193	0.206	0.029	0.111	0.172	0.124
Sandy clay loam	3	0.367	0.428	0.046	0.136	0.530	0.388
Silty loam	3	0.241	0.263	0.034	0.131	0.274	0.206
Clay loam	7	0.270	0.280	0.062	0.209	0.282	0.206
Clay	7	0.245	0.266	0.038	0.177	0.259	0.190
Sandy clay loam	7	0.561	0.614	0.095	0.204	0.815	0.587
Silty loam	7	0.343	0.364	0.052	0.205	0.416	0.310
Clay loam	10	0.311	0.322	0.077	0.242	0.341	0.245
Clay	10	0.286	0.296	0.045	0.212	0.306	0.226
Sandy clay loam	10	0.673	0.723	0.178	0.294	0.978	0.713
Silty loam	10	0.404	0.421	0.065	0.248	0.499	0.367
Clay loam	20	0.391	0.406	0.111	0.342	0.478	0.348
Clay	20	0.366	0.377	0.068	0.291	0.435	0.315
Sandy clay loam	20	0.951	0.985	0.345	0.436	1.404	1.011
Silty loam	20	0.534	0.566	0.103	0.353	0.717	0.516
Clay loam	30	0.456	0.472	0.147	0.418	0.595	0.432

Clay	30	0.424	0.431	0.085	0.356	0.538	0.387
Sandy clay loam	30	1.191	1.202	0.412	0.578	1.736	1.256
Silty loam	30	0.643	0.676	0.136	0.442	0.877	0.645
Clay loam	90	0.735	0.746	0.284	0.748	1.044	0.774
Clay	90	0.644	0.653	0.188	0.625	0.958	0.695
Sandy clay loam	90	2.026	2.067	0.624	1.297	3.106	2.276
Silty loam	90	1.103	1.128	0.466	0.832	1.565	1.144
Clay loam	160	0.969	0.976	0.426	1.021	1.426	1.065
Clay	160	0.822	0.832	0.336	0.846	1.300	0.956
Sandy clay loam	160	2.744	2.775	0.875	2.108	4.421	3.146
Silty loam	160	1.483	1.500	0.689	1.183	2.138	1.570
Clay loam	200	1.072	1.087	0.558	1.168	1.612	1.21
Clay	200	0.911	0.919	0.456	0.954	1.472	1.084
Sandy clay loam	200	2.945	3.081	0.998	2.442	4.799	3.578
Silty loam	200	1.66	1.683	0.785	1.364	2.415	1.781
Clay loam		R^2 **RMSE**	0.999 0.042	0.972 1.152	0.998 0.081	0.999 0.608	0.998 0.025
Clay		R^2 **RMSE**	0.999 0.037	0.929 1.138	0.997 0.160	0.997 0.605	0.996 0.003
Sandy clay loam		R^2 **RMSE**	0.999 0.180	0.989 3.272	0.993 1.758	0.997 2.523	0.996 0.562
Silty loam		R^2 **RMSE**	0.999 0.085	0.978 1.697	0.997 0.710	0.999 1.005	0.999 0.031

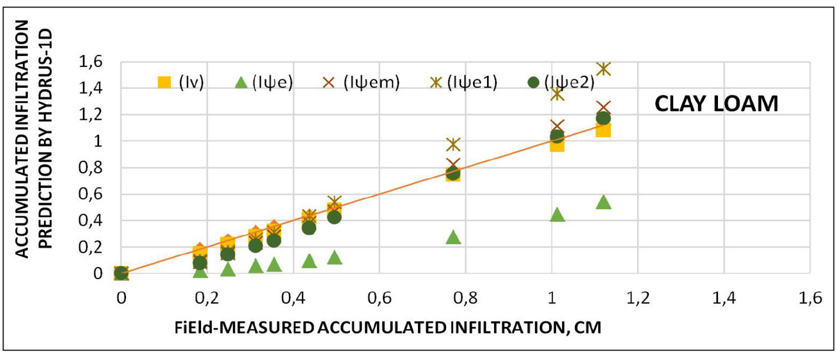

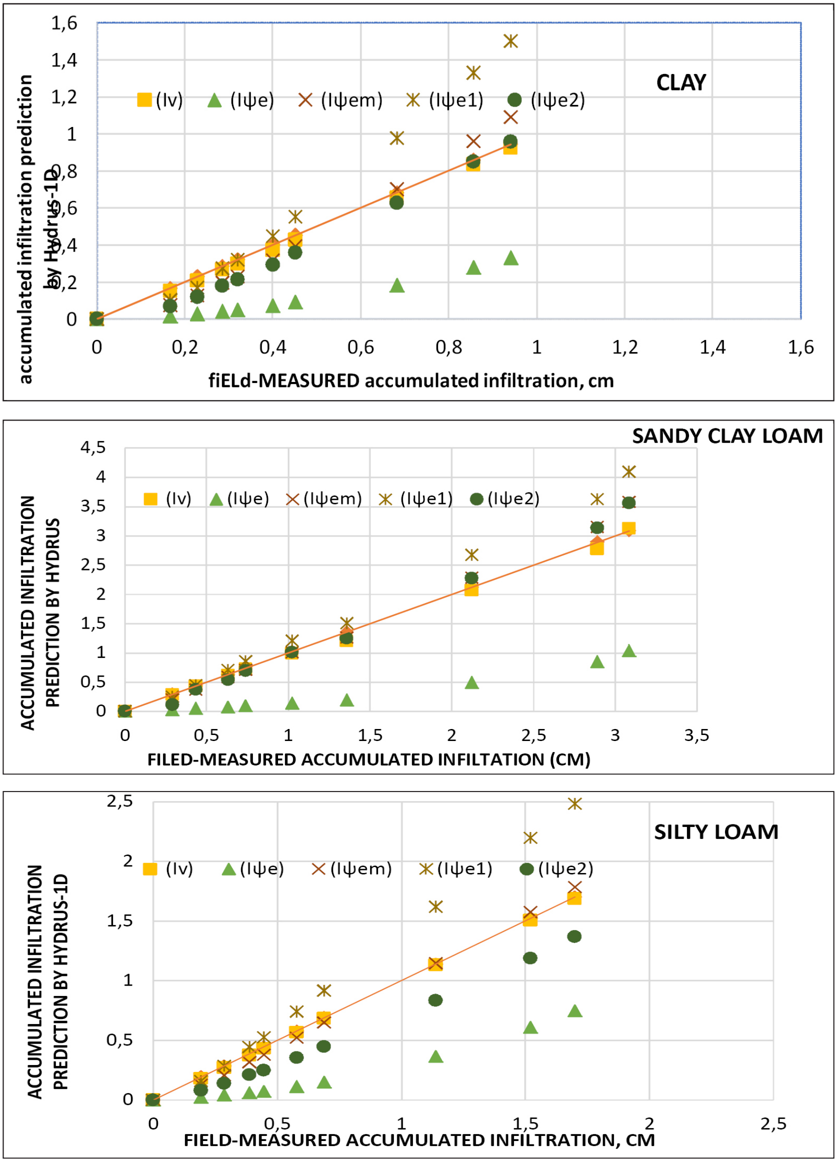

Fig. 1. The relationship between the accumulative infiltration measured in the field and the one predicted by the Hydrus-1D

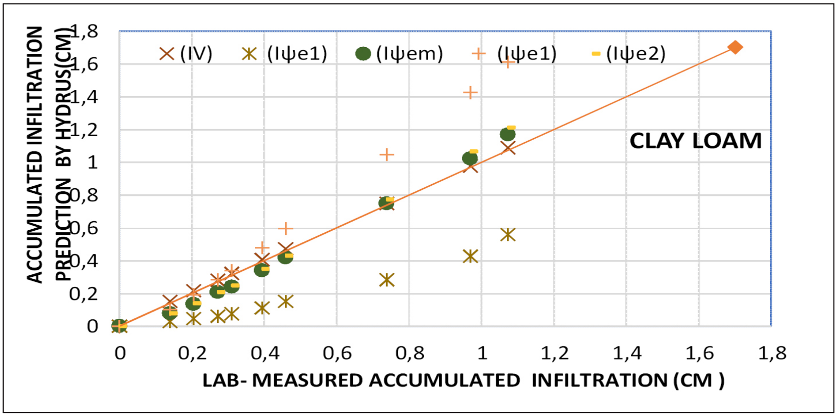
ACCUMULATED INFILTRATION PREDICTION BY HYDRUS(CM)
(IV) (Iψe1) (Iψem) (Iψe1) (Iψe2)
CLAY LOAM
0 0,2 0,4 0,6 0,8 1 1,2 1,4 1,6 1,8
LAB- MEASURED ACCUMULATED INFILTRATION (CM)

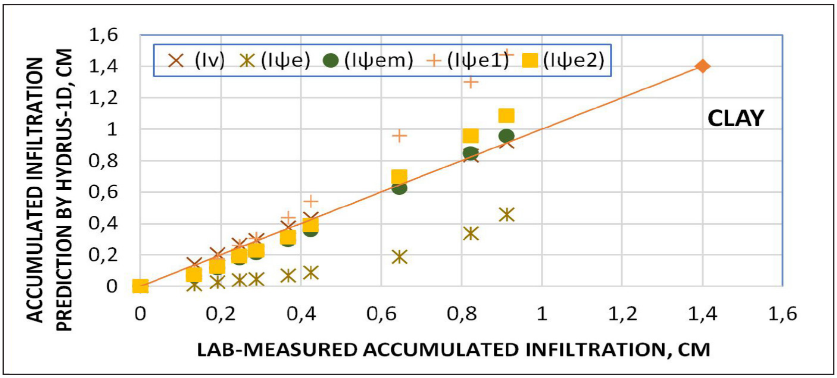
ACCUMULATED INFILTRATION PREDICTION BY HYDRUS-1D, CM
(Iv) (Iψe) (Iψem) (Iψe1) (Iψe2)
CLAY
0 0,2 0,4 0,6 0,8 1 1,2 1,4 1,6
LAB-MEASURED ACCUMULATED INFILTRATION, CM

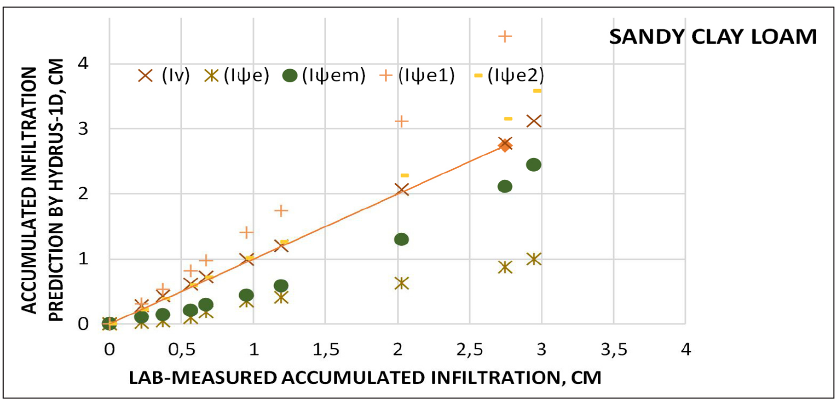
ACCUMULATED INFILTRATION PREDICTION BY HYDRUS-1D, CM
SANDY CLAY LOAM
(Iv) (Iψe) (Iψem) (Iψe1) (Iψe2)
0 0,5 1 1,5 2 2,5 3 3,5 4
LAB-MEASURED ACCUMULATED INFILTRATION, CM

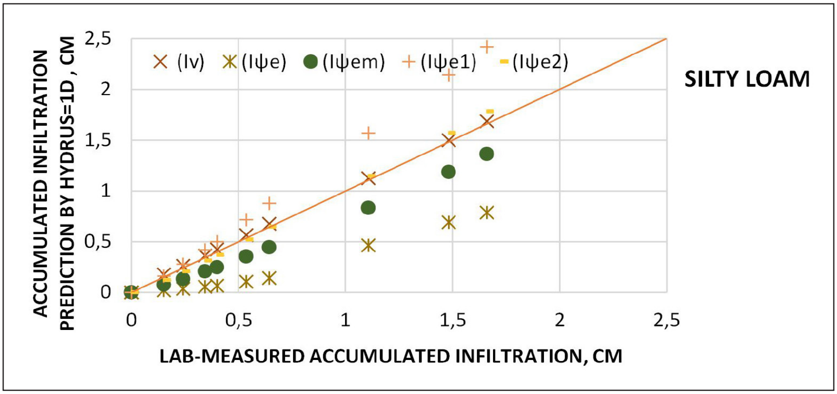

Fig. 2. The relationship between the accumulative infiltration measured in the laboratory and the one predicted by the Hydrus-1D software

Conclusion

This study highlights the importance of measuring accumulated infiltration values, as they are crucial to understanding soil water dynamics. Given the challenges associated with direct measurement, the Hydrus-1D program provides an effective predictive tool. It has been used to predict the infiltration value depending on simpler characteristics in the measurement process such as moisture content at saturation or residual moisture content in comparison with the measured values of the infiltration in the field and in the laboratory.

In this study we recommend modifying the air entry value according to the models used in order to improve the performance of the Hydrus-1D program to predict the accumulative infiltration values, especially adopting the modified formula in this study in order to obtain the best values and the lowest percentage of error. The study recommends using the inverse of the air entry value to predict other hydraulic properties, such as unsaturated hydraulic conductivity and diffusivity, which are challenging to measure.

Acknowledgment. The authors are very grateful to the University of Mosul / college of Agriculture and Forestry for their provided facilities, which helped to improve the quality of this work.

References

1. Simunek, J., Neumann, L.E., & Cook, F.J. (2011). Implementation of quadratic upstream interpolation schemes for solute transport into HYDRUS-1D. *Envi-*

ronmental Modeling and Software, 26(11), 1298-1308. https://doi.org/10.1016/j.envsoft.2011.05.010

2. Rezaei, M., Seuntjens, P., Shahidi, R., Joris, I., Boenne, W., Al-Barri, B., & Cornelis, W.M. (2016). The relevance of in situ and laboratory characterization of sandy soil hydraulic properties for soil water simulations. *Journal of Hydrology, 534*, 251-265. https://doi.org/10.1016/j.jhydrol.2015.12.062
3. Kasel, D., Bradford, S.A., Simunek, J., Heggen, M., Vereecken, H., & Klumpp, E. (2013). Transport and retention of multi-walled carbon nanotubes in saturated porous media: Effects of input concentration and grain size. *Water Research, 47*(2), 933-944. https://doi.org/10.1016/j.watres.2012.11.019
4. Dabach, S., Lazarovitch, N., Simunek, J., & Shani, U. (2013). Numerical investigation of irrigation scheduling based on soil water status. *Irrigation Science, 31*(1), 27-36. https://link.springer.com/article/10.1007/s00271-011-0289-x EDN: https://elibrary.ru/qgiygv
5. Esam, M., AL-Qassab, S.A., & AL-Wazzan, F.A. (2022). Using inverse modeling by HYDRUS-1D to predict some soil hydraulic parameters from soil water evaporation. *Colombia Forestal, 25*, 21-35. https://doi.org/10.14483/2256201X.18157
6. Mustafa, B.M., & Al-Wazzan, F.A. (2022). The variation of some soil physical properties by using water with different salinities. *Int. J. Agricult. Stat. Sci., 18*(1), 2099-2110. https://connectjournals.com/pages/articledetails/toc036676
7. Al-Wazzan, F.A., & Sarbast, A.M. (2022). Effects of conservation and conventional tillage on some soil hydraulic properties. *IOP Conf. Series: Earth and Environmental Science, 1060*, 012002. https://doi.org/10.1088/1755-1315/1060/1/012002 EDN: https://elibrary.ru/yyyyzs
8. Philip, J.R. (1957a). The theory of infiltration. 1: The infiltration equation and its solution. *Soil Sci., 83*, 345-357. https://journals.lww.com/soilsci/Citation/1957/05000/THE_THEORY_OF_INFILTRATION_1_THE_INFILTRATION.2.aspx
9. Klute, A. (1986). Methods of soil analysis part 1: Physical and mineralogical methods (2nd ed.). *Agronomy Monograph No.9*. Madison, WI: ASA-SSSA. https://doi.org/10.2136/sssabookser5.1.2ed
10. Parr, J.F., & Bertrand, A.R. (1960). Water infiltration into soils. *Adv. In Agron, 12*, 311-363. https://doi.org/10.1016/S0065-2113(08)60086-3
11. Lenhard, R., Parker, J.C., & Mishra, S. (1989). On the correspondence between Brooks-Corey and van Genuchten model. *J. Irrig. Drain. E., 115*, 744-751. https://doi.org/10.1061/(ASCE)0733-9437(1989)115:4(744)
12. Cornelis, V.M., Khlosi, M., Hartmann, R., van Meirvenne, M., & Devos, B. (2005). Comparison on unimodal analytical expression for soil water reten-

tion curve. *Soil Sci. Soc. Am. J., 69*, 1902-1911. https://journals.lww.com/soilsci/abstract/2012/06000/entropy_characterization_of_soil_pore_systems.1.aspx
13. van Genuchten, M.Th. (1980). A closed-form equation for predicting the hydraulic conductivity of unsaturated soil. *Soil Sci. Soc. Am. J., 44*, 892-898. https://doi.org/10.2136/sssaj1980.036159950
14. Philip, J.R. (1957b). The theory of infiltration. 2: The profile of infinity. *Soil Sci., 83*, 345-448. https://journals.lww.com/soilsci/Citation/1957/06000/The_Theory_of_Infiltration__2__the_Profile_of.3.aspx
15. Hillel, D. (1980). *Applications of soil physics*. Academic press, New York.
16. Ritter, A., Hupet, F., Munoz-Carpena, R., Lambot, S., & Vanclooster, M. (2003). Using inverse method for estimating soil hydraulic properties from field data as an alternative to direct methods. *Agricultural Water Management, 59*, 77-96. https://doi.org/10.1016/S0378-3774(02)00160-9 EDN: https://elibrary.ru/bfwujr
17. Hachimi, M., Maslouhi, A., Tamoh, K., & Qanza, H. (2019). Estimation of soil hydraulic properties of basin Loukkos (Morocco) by inverse modeling. *KSCE Journal of Civil Engineering, 23*(3), 1407-1419. https://doi.org/10.1007/s12205-019-0628-7
18. Dexter, A.R., & Richard, G.R. (2009). Tillage of soil in relation to their bimodal pore size distributions. *Soil Tillage Res., 103*, 113-118. https://doi.org/10.1016/j.still.2008.10.001
19. Schaap, M.G., Leij, F.J., & van Genuchten, M.Th. (2001). Rosetta: a computer program for estimating soil hydraulic parameters with hierarch pedotransfer functions. *Journal of Hydrology, 251*(3-4), 163-176. https://doi.org/10.1016/S0022-1694(01)00466-8 EDN: https://elibrary.ru/arbjnj
20. Simunek, J., Angulo-Jaramillo, R., Schaap, M.G., Martinus, J.V., & Van Genuchten, Th. (1998). Using an inverse method to estimate the hydraulic properties of crusted soil from tension-disc infiltrometer data. *Geoderma, 86*, 61-81. https://doi.org/10.1016/S0016-7061(98)00035-4 EDN: https://elibrary.ru/absmkd
21. Vogel, T., van Genuchten, M.Th., & Cislerova, M. (2001). Effect of the shape of the soil hydraulic functions near saturation on variably-saturated flow predictions. *Advances in Water Resources, 24*, 133-144. https://doi.org/10.1016/S0309-1708(00)00037-3
22. Mualem, Y. (1976). A new model predicting the hydraulic of unsaturated porous media. *Water Resour. Res., 12*(3), 513-522. https://doi.org/10.1029/WR012i003p00513

23. Brooks, R.H., & Corey, A.T. (1964). Hydraulic properties of porous media. *Hydrology paper No.3*. Civil Engineering Department, Colorado State University, Fort Collins. https://api.mountainscholar.org/server/api/core/bitstreams/f7532f39-5f13-4e4b-a3c0-dd9523ba5219/content

DATA ABOUT THE AUTHOR

Faris A. Al-Wazzan

Department of Soil Science and Water Resources,
College of Agriculture and Forestry, University of Mosul
Mosul, Iraq
Dr.farisakram@uomosul.edu.iq

Поступила 02.05.2024 Received 02.05.2024
После рецензирования 25.11.2024 Revised 25.11.2024
Принята 05.12.2024 Accepted 05.12.2024